



## Special Feature: Power Semiconductor Devices

Research Report

### Ultra-low Feedback Capacitance SiC JFET for High-frequency Operation

Tsuyoshi Ishikawa, Katsuya Nomura, Yasunori Tanaka, Tsutomu Yatsuo and Koji Yano

Report received on Aug. 5, 2015

**■ABSTRACT■** We propose a novel SiC vertical junction field-effect transistor (VJFET) with low feedback capacitance  $C_{rss}$ . A key feature of the proposed device is a  $p^+$  screen grid inserted between the gate and drain electrodes, which is effective at reducing  $C_{rss}$  by 80% compared with a conventional VJFET. Due to the low  $C_{rss}$ , the proposed device has a faster switching speed and lower total power loss than any existing SiC transistor. We estimate that the carrier frequency of a DC/DC converter with the new type of VJFET can be increased more than two-fold compared to that with a trench gate MOSFET. Moreover, based on the low  $C_{rss}$ , we believe that the proposed device will enable high-frequency operation of power conversion systems and contribute to the miniaturization of power control units (PCUs) for HVs and EVs.

**■KEYWORDS■** Silicon Carbide (SiC), Power Semiconductor Devices, JFET, Feedback Capacitance, Switching Loss, Power Conversion System

#### 1. Introduction

Power semiconductor switching devices are used in power conversion systems for the motor drive of hybrid electric vehicles (HV) and electric vehicles (EV). Currently, bipolar devices such as Si IGBTs and Si PiN diodes are mainly used as the switching devices. While minority carriers play an important role in reducing the on-state voltage drop in these Si bipolar power devices, they also contribute to the tail current and reverse recovery current to increase the switching loss. Therefore, there is a trade-off between the on-state voltage drop and switching loss. In order to resolve this issue, methods for carrier lifetime control, which introduce recombination centers by metal diffusion and charged particle beam irradiation,<sup>(1-3)</sup> have been investigated. Recently, because further improvement in the performance of Si bipolar power devices has been recognized as difficult, new technologies to overcome the limitations of Si materials are in high demand.

Silicon carbide (SiC) is a promising material for next generation power semiconductor devices because of its large critical breakdown electric field, high operating temperature and superior thermal conductivity. In particular, the large critical electric field makes it possible to increase the doping concentration and

decrease the thickness of the voltage-sustaining layer (drift region) to maintain a breakdown voltage equivalent to that of conventional Si power devices. Therefore, even unipolar devices such as JFETs, MOSFETs and Schottky barrier diodes can achieve lower on-state voltage drop (on-resistance) in the case of SiC power devices. The switching loss of these devices is considerably low compared with Si IGBTs and Si PiN diodes because there is no tail current or reverse recovery current. A lower switching loss enables high-frequency operation of power conversion systems to keep the total power dissipation low and extends the driving range of HVs and EVs. High-frequency operation allows the miniaturization of power control units (PCUs) and in particular of passive components such as inductors and capacitors in the DC/DC converter (**Fig. 1**). Downsizing of the PCU is valuable because this provides greater flexibility for its installation and enables alternate layouts of a vehicle. We believe that SiC power devices will contribute to boosting the performance of HVs and EVs.

In this paper, we focus on the switching loss of SiC transistors that becomes apparent during high-frequency operation of power conversion systems and propose a novel SiC transistor that has lower switching loss.<sup>(4,5)</sup> In order to reduce the switching loss, it is necessary to rapidly switch between the on

and off states. High-speed switching can be achieved by reducing the feedback capacitance  $C_{r_{SS}}$ , which has to charge during the switching transient. We have therefore chosen to base our proposed low- $C_{r_{SS}}$  transistor on SiC vertical JFETs (VJFETs) because they already have demonstrated low on-resistance<sup>(6-9)</sup> as well as no reliability or long-term stability concerns.<sup>(10,11)</sup> The proposed transistor adopts part of the structure of SiC buried gate static induction transistors (BGSITs),<sup>(8,9)</sup> a type of VJFET for which an extremely low on-resistance is easy to achieve.

**2. Device Structure and Simulation**

A schematic of the proposed VJFET, which we call a Screen Grid VJFET (SG-VJFET), is shown in **Fig. 2**. A major feature of the SG-VJFET is a p<sup>+</sup> screen grid, which is made of p-type SiC and is located between the buried p<sup>+</sup> gate and drain electrodes. This transistor usually operates with the screen grid electrode short-circuited to the source electrode. The screen grid weakens the capacitive coupling between the gate and drain to reduce  $C_{r_{SS}}$ . On the other hand, it also restricts the current flow to narrow regions, which increases the on-resistance. In order to suppress this effect, a current spreading layer, which is an n-type high impurity concentration layer, is introduced between the p<sup>+</sup> gate and screen grid.

To compare the performance of the SG-VJFET with that of other SiC FETs, device modeling of a trench VJFET (Tr. VJFET) and trench gate MOSFET

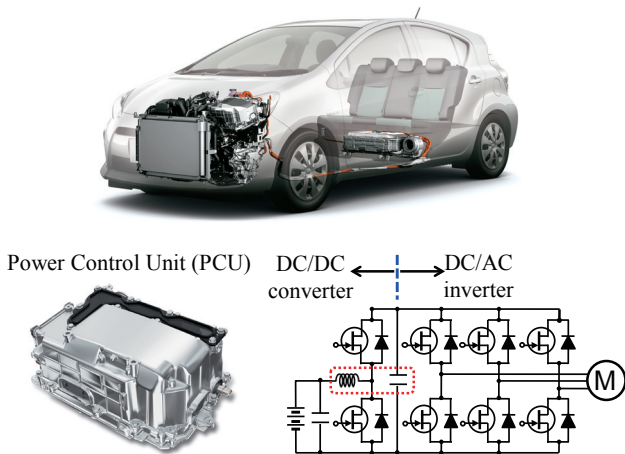
(Tr. MOSFET) was carried out with a device simulator using published data.<sup>(6,7,12)</sup> The thickness and doping concentration of the voltage-sustaining layer (n<sup>-</sup> drift layer) and n<sup>+</sup> substrate were made common among the three devices (n<sup>-</sup> drift layer: 10 μm, 8 × 10<sup>15</sup> cm<sup>-3</sup>. n<sup>+</sup> substrate: 350 μm, 6 × 10<sup>18</sup> cm<sup>-3</sup>). For the SG-VJFET, the n<sup>+</sup> channel region was doped to slightly above 10<sup>16</sup> cm<sup>-3</sup> and the p<sup>+</sup> gate region was doped to 2 × 10<sup>19</sup> cm<sup>-3</sup>. For the Tr. MOSFET, we assumed an inversion channel mobility of 120 cm<sup>2</sup>/V·s, which seems to be the best mobility currently available for this type of device.<sup>(13)</sup> A summary of the device structure and the static characteristics of the SiC FETs at room temperature are provided in **Table 1**.

To compare the dynamic characteristics of the SG-VJFET with that of the Tr. VJFET and Tr. MOSFET, a double-pulse clamped inductive load test was performed with test circuit shown in **Fig. 3**. The size of all transistors was the same (active area: 0.25 cm<sup>2</sup>) to allow for comparison. A 650 VDC voltage was supplied to an inductor of 100 μH and a freewheeling SiC Schottky barrier diode (SiC SBD) with an active area of 0.25 cm<sup>2</sup>. The total stray inductance  $L_s$  in the bus voltage path was set to 60 nH.

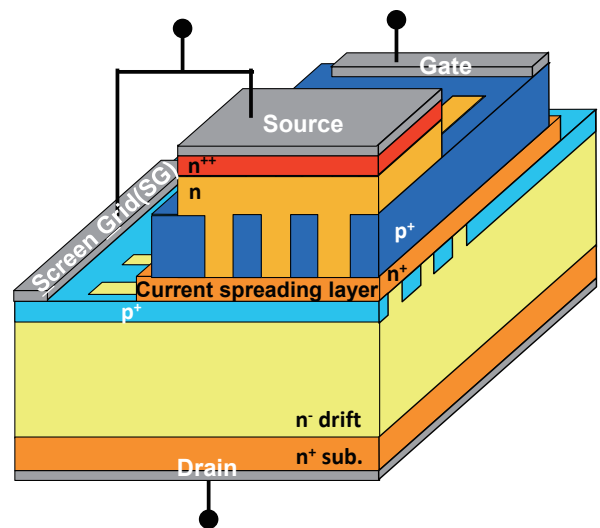
**3. Results and Discussion**

**3.1 Static Characteristics**

The static characteristics of the SG-VJFET were calculated using the device simulator. The

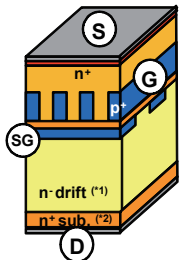
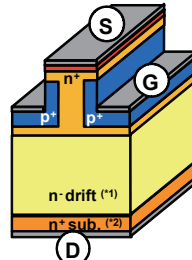
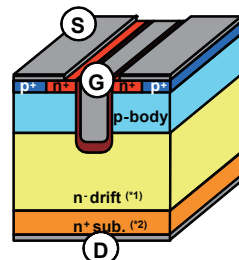


**Fig. 1** Power conversion system for hybrid electric vehicles (HVs). Power control unit consists of DC/DC converters, DC/AC inverters, passive components and liquid cooling system.



**Fig. 2** A schematic diagram of the proposed SiC VJFET structure (Screen Grid vertical JFET: SG-VJFET).

**Table 1** Summary of static characteristics for different types of SiC transistors.

	(Proposed device) SG-VJFET	Tr. VJFET	Tr. MOSFET
Device structure			
Specific on-resistance $R_{onA}$ @ $V_{DS} = 1.0$ V	2.4 m $\Omega$ ·cm <sup>2</sup> (*3)	3.3 m $\Omega$ ·cm <sup>2</sup> (*3)	2.7 m $\Omega$ ·cm <sup>2</sup> (*4)
Threshold voltage $V_{th}$ @ $V_{DS} = 0.1$ V, $I_D = 0.1$ A/cm <sup>2</sup>	+ 1.0 V	+ 1.0 V	+ 6.1 V
Feedback capacitance $C_{rss}$ @ $V_{DS} = 650$ V	0.19 nF/cm <sup>2</sup>	0.97 nF/cm <sup>2</sup>	0.38 nF/cm <sup>2</sup>

(\*1) n<sup>-</sup> drift layer: 8 × 10<sup>15</sup> cm<sup>-3</sup>, 10 μm (\*3) @  $V_{GS} = 2.5$  V  
 (\*2) n<sup>+</sup> substrate: 6 × 10<sup>18</sup> cm<sup>-3</sup>, 350 μm (\*4) @  $V_{GS} = 15$  V

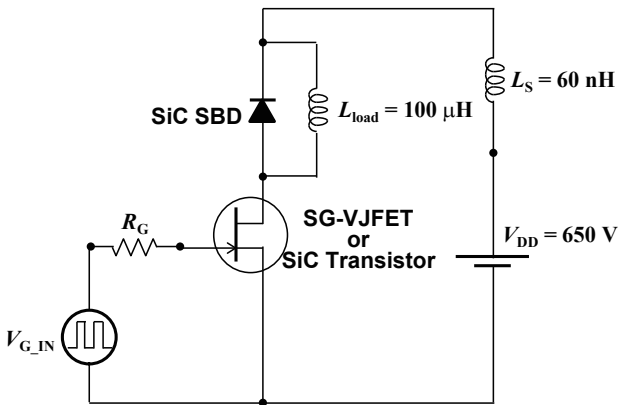


**Fig. 3** Diagram of a standard inductive load test circuit to evaluate the dynamic characteristics of the three transistors.

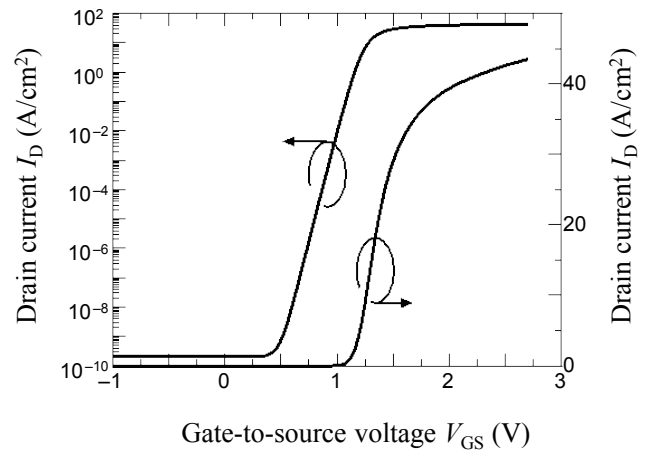


**Fig. 4** Simulated transfer characteristic ( $I_D$  vs.  $V_{GS}$ ) of SG-VJFET.

calculated transfer characteristic ( $I_D$  vs.  $V_{GS}$ ) is shown in **Fig. 4**. A positive threshold voltage  $V_{th}$  of 1.0 V (@  $V_{DS} = 0.1$  V,  $I_D = 0.1$  A/cm<sup>2</sup>) was achieved, confirming the normally-off operation of the SG-VJFET. The calculated output characteristics ( $I_D$  vs.  $V_{DS}$ ) are shown in **Fig. 5**. A specific on-resistance  $R_{onA}$  (@  $V_{GS} = 2.5$  V,  $V_{DS} = 1.0$  V) of 2.4 m $\Omega$ ·cm<sup>2</sup> was achieved due to the fine line-and-space p<sup>+</sup> gate pattern. As shown in **Fig. 6**, a blocking voltage of more than 1500 V was achieved even at zero gate bias (i.e.,  $V_{GS} = 0$  V). **Figure 7** shows

a comparison of  $C_{rss}$  for the three SiC transistors, which was smallest for the SG-VJFET and 80% lower than that of conventional VJFETs. It is therefore clear that the screen grid is effective at reducing  $C_{rss}$ .

### 3.2 Dynamic Characteristics

To confirm the improvement in the dynamic characteristics of the SG-VJFET, a double-pulse test was performed on the three SiC transistors. The gate input voltage swing of the Tr. MOSFET

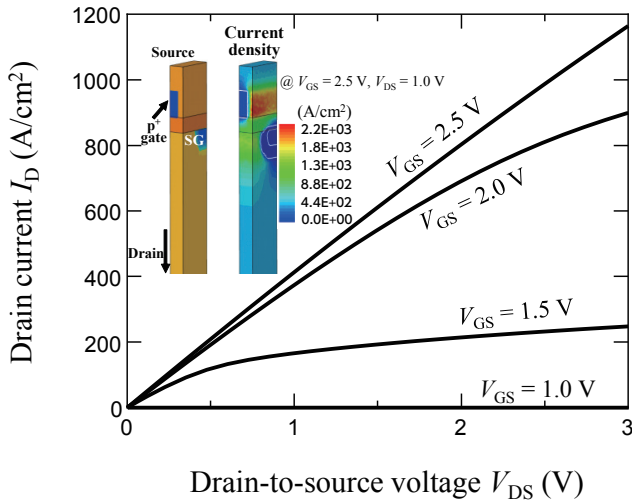


Fig. 5 Simulated output characteristic ( $I_D$  vs.  $V_{GS}$ ) of SG-VJFET at  $V_{GS} = 1.0$ - $2.5$  V.

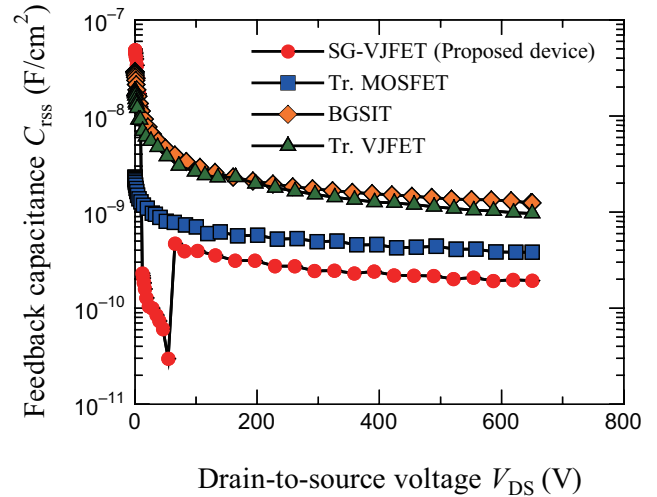


Fig. 7 Comparison of simulated feedback capacitance  $C_{iss}$  among three different types of SiC transistors.

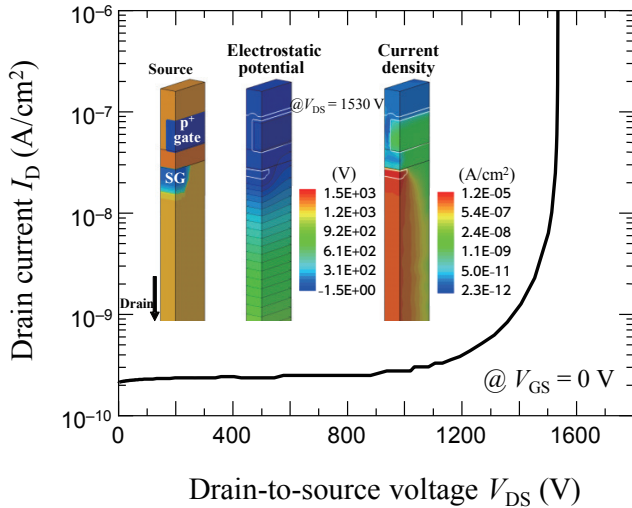


Fig. 6 Simulated forward blocking characteristic of SG-VJFET at  $V_{GS} = 0$  V.

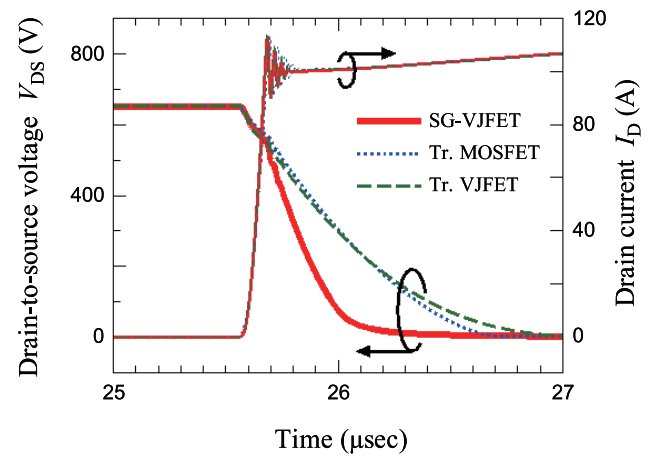


Fig. 8 Simulated turn-on switching waveforms of three different transistors. ( $V_{DD} = 650$  V,  $I_D = 100$  A)

was  $V_{G\_IN(off)} = 0$  V to  $V_{G\_IN(on)} = 15$  V and that of both the SG-VJFET and Tr. VJFET was  $V_{G\_IN(off)} = -5$  V to  $V_{G\_IN(on)} = 2.5$  V. In order to easily evaluate the performance with only a comparison of the fall and rise rates  $dv/dt$  of the drain voltage  $V_{DS}$  during the turn-on and turn-off transient, the current rise and fall rates  $di/dt$  were adjusted to be the same for all three transistors.

The turn-on and turn-off waveforms at 650 V and 100 A are shown in Figs. 8 and 9, respectively. Due to the low  $C_{iss}$  of the SG-VJFET, its turn-on switching speed was the fastest among the three devices, as is apparent from Fig. 8. The turn-on switching loss  $E_{on}$

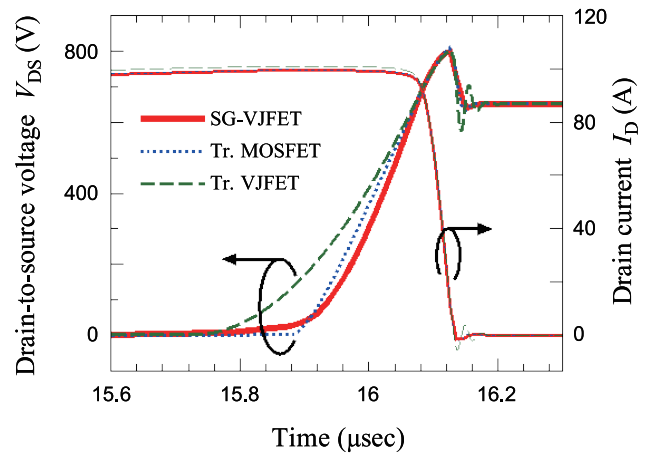
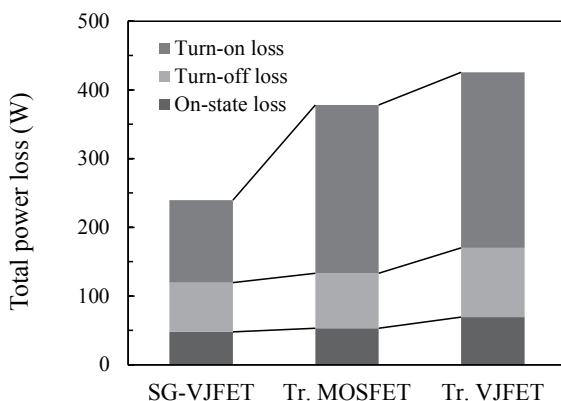


Fig. 9 Simulated turn-off switching waveforms of three different transistors. ( $V_{DD} = 650$  V,  $I_D = 100$  A)

was reduced by 50% and 60% compared with the Tr. MOSFET and Tr. VJFET, respectively. As shown in Fig. 9, the rise rates  $dv/dt$  of the SG-VJFET and Tr. MOSFET were roughly the same during the turn-off transient. The effect of reducing  $C_{rss}$  on the increase in  $dv/dt$  was small compared with the turn-on transient, and it is said that  $dv/dt$  typically depends on the gate-to-source capacitance  $C_{gs}$  during the turn-off transient.<sup>(14)</sup> Nevertheless, the turn-off switching speed of the SG-VJFET was the fastest among the three devices. The turn-off switching loss  $E_{off}$  of the SG-VJFET was 10% and 45% lower than that of the Tr. MOSFET and Tr. VJFET, respectively.

### 3.3 Total Power Dissipation

The total power dissipation (the sum of  $E_{on}$ ,  $E_{off}$  and the conduction loss  $E_{cond}$ ) of each FET was estimated from the simulated static and dynamic characteristics, assuming that the converter carrier frequency and duty ratio were 10 kHz and 0.5, respectively.  $E_{on}$  and  $E_{off}$  were calculated under the same  $di/dt$  conditions (i.e., the same surge voltage  $\Delta V_{surge}$ ) taking into account noise due to electromagnetic interference and the breakdown voltage. The total power dissipation of the SG-VJFET was the lowest among existing SiC power devices (Fig. 10). Based on this estimation, the carrier frequency  $f_c$  of a DC/DC converter with an SG-VJFET can be increased more than two-fold compared with that using a Tr. MOSFET to maintain the same dissipation (Fig. 11). Based on these results, we believe that the SG-VJFET is suitable for fast switching applications.



**Fig. 10** Comparison of FET total power loss among three different transistors. (Switching current: 400 A/cm<sup>2</sup>)

## 4. Conclusion

We propose a novel SiC VJFET with low feedback capacitance  $C_{rss}$  based on results obtained with a device simulator. A key feature of the proposed VJFET is a p<sup>+</sup> screen grid inserted between the gate and drain electrodes, which is effective at reducing  $C_{rss}$  by 80% compared with that of conventional VJFETs. Due to the low  $C_{rss}$ , the total power loss of the proposed SG-VJFET is lower than that for any existing SiC transistor. Based on these results, we believe this device will enable high-frequency operation of power conversion systems and contribute to the miniaturization of PCUs for HVs and EVs.

## References

- (1) Vobecký, J. and Hazdra, P., "Low-temperature Radiation Controlled Diffusion of Palladium and Platinum in Silicon for Advanced Lifetime Control", *Nucl. Instrum. Methods Phys. Res. B*, Vol. 253, No. 1-2 (2006), pp. 162-166.
- (2) Hazdra, P., Vobecký, J., Dorschner, H. and Brand, K., "Axial Lifetime Control in Silicon Power Diodes by Irradiation with Protons, Alphas, Low- and High-energy Electrons", *Microelectron. J.*, Vol. 35, No. 3 (2004), pp. 249-257.
- (3) Hazdra, P. and Komarnitsky, V., "Lifetime Control in Silicon Power P-i-N Diode by Ion Irradiation: Suppression of Undesired Leakage", *Microelectron. J.*, Vol. 37, No. 3 (2006), pp. 197-203.
- (4) Ishikawa, T., Nomura, K., Sugiyama, T., Uesugi, T., and Nishikawa, K., "A New Type of SiC-VJFET"

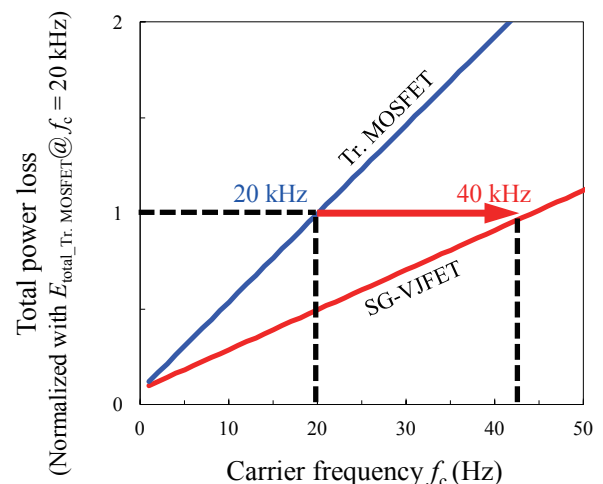


**Fig. 11** Dependence of total power loss on carrier frequency  $f_c$ . Each data is normalized with total loss of trench-gate MOSFET at  $f_c = 20$  kHz.

with Extreme Low Feedback Capacitance”, *Proc. of 25th Int. Symp. Power Semiconductor Devices & ICs* (2013), pp. 183-186.

- (5) Ishikawa, T., Tanaka, Y., Yatsuo, T. and Yano, K., “SiC Power Devices for HEV/EV and a Novel SiC Vertical JFET”, *Tech. Digest of Int. Electron Devices Meeting* (2014), pp. 2.2.1-2.2.4.
- (6) Sheridan, D. C., Ritenour, A., Bondarenko, V., Burks, P. and Casady, J. B., “Record 2.8 mΩ-cm<sup>2</sup> 1.9 kV Enhancement-mode SiC VJFETs”, *Proc. of 21st Int. Symp. Power Semiconductor Devices & ICs* (2009), pp. 335-338.
- (7) Ritenour, A., Sheridan, D. C., Bondarenko, V. and Casady, J. B., “Performance of 15 mm<sup>2</sup> 1200 V Normally-off SiC VJFETs with 120 A Saturation Current”, *Mat. Sci. Forum*, Vol. 645-648 (2010), pp. 937-940.
- (8) Tanaka, Y., Okamoto, M., Takatsuka, A., Arai, K., Yatsuo, T., Yano, K. and Kasuga, M., “700-V 1.0-mΩ-cm<sup>2</sup> Buried Gate SiC-SIT (SiC-BGSIT)”, *IEEE Electron Device Lett.*, Vol. 27 (2006), pp. 908-910.
- (9) Takatsuka, A., Tanaka, Y., Yano, K., Yatsuo, T. and Arai, K., “980 V, 33 A Normally-off 4H-SiC Buried Gate Static Induction Transistors”, *Mat. Sci. Forum*, Vol. 679-680 (2011), pp. 662-665.
- (10) Speer, K. M., Chatty, K., Bondarenko, V., Sheridan, D. C., Matocha, K. and Casady, J. B., “Demonstration of SiC Vertical Trench JFET Reliability”, *Mat. Sci. Forum*, Vol. 717-720 (2012), pp. 1017-1020.
- (11) Lawson, K., Alvarez, G., Bayne, S. B., Veliadis, V., Ha, H. C., Urciuoli, D. and Scozzie, C., “Reliable Operation of 1200-V SiC Vertical Junction-field-effect-transistor Subjected to 16,000-pulse Hard Switching Stressing”, *Mat. Sci. Forum*, Vol. 717-720 (2012), pp. 1021-1024.
- (12) Nakano, Y., Nakamura, R., Sakairi, H., Mitani, S. and Nakamura, T., “690 V, 1.00 mΩcm<sup>2</sup> 4H-SiC Double-trench MOSFETs”, *Mat. Sci. Forum*, Vol. 717-720 (2012), pp. 1069-1072.
- (13) Nanen, Y., Kato, M., Suda, J. and Kimoto, T., “Effects of Nitridation on 4H-SiC MOSFETs Fabricated on Various Crystal Faces”, *IEEE Trans. Electron Devices*, Vol. 60, No. 3 (2013), pp. 1260-1262.
- (14) Baliga, B. J., *Fundamentals of Power Semiconductor Devices* (2008), p. 442, Springer.

Figs. 1, 2, 4-11 and Table 1

Reprinted from *Tech. Digest of Int. Electron Devices Meeting* (2014), pp. 2.2.1-2.2.4, Ishikawa, T., Tanaka, Y., Yatsuo, T. and Yano, K., SiC Power Devices for HEV/EV and a Novel SiC Vertical JFET, © 2014 IEEE, with permission from IEEE.

---

### Tsuyoshi Ishikawa

Research Fields:

- Power Semiconductor Devices
- Power Electronics

Academic Degree: Dr.Eng.

Academic Societies:

- IEEE
- The Japan Society of Applied Physics




---

### Katsuya Nomura

Research Fields:

- Power Semiconductor Devices
- Power Electronics

Academic Societies:

- The Institute of Electrical Engineers of Japan
- The Institute of Electronics, Information and Communication Engineers




---

### Yasunori Tanaka\*

Research Fields:

- Semiconductor Devices
- Power Electronics

Academic Degree: Ph.D.

Academic Societies:

- The Japan Society of Applied Physics
- The Institute of Electrical Engineers of Japan

Awards:

- The William M. Portnoy Award at the Energy Conversion Congress and Exposition (2010)
- 26th Int. Symp. Power Semiconductor Devices & ICs Best Paper Award, 2014




---

### Tsutomu Yatsuo\*

Research Fields:

- Semiconductor Devices
- Power Electronics

Academic Degree: Dr.Eng.

Academic Society:

- The Institute of Electrical Engineers of Japan

Award:

- 26th Int. Symp. Power Semiconductor Devices & ICs Best Paper Award, 2014




---

### Koji Yano\*\*

Research Field:

- Design of Silicon and Compound Power Semiconductor Devices

Academic Degree: Dr.Eng.

Academic Societies:

- IEEE
- The Institute of Electrical Engineers of Japan
- The Japanese Society of Applied Physics



\* National Institute of Advanced Industrial Science and Technology

\*\* University of Yamanashi